NeuroImage 188 (2019) 217–227

Contents lists available at ScienceDirect

NeuroImage

journal homepage: www.elsevier.com/locate/neuroimage

Reduced white matter fractional anisotropy mediates cortical thickening in adults born preterm with very low birthweight

Lars M. Rimol [a,b,c,*], Violeta L. Botellero [a,d], Knut J. Bjuland [e], Gro C.C. Løhaugen [e], Stian Lydersen [f], Kari Anne I. Evensen [a,i], Ann-Mari Brubakk [a], Live Eikenes [c], Marit S. Indredavik [a], Marit Martinussen [a,g], Anastasia Yendiki [j], Asta K. Håberg [b,h], Jon Skranes [a,e]

[a] Department of Clinical and Molecular Medicine, Faculty of Medicine and Health Sciences, Norwegian University of Science and Technology (NTNU), Trondheim, Norway
[b] Norwegian Advisory Unit for Functional MRI, Department of Radiology, St. Olavs Hospital, Trondheim University Hospital, Trondheim, Norway
[c] Department of Circulation and Medical Imaging, Faculty of Medicine and Health Sciences, NTNU, Trondheim, Norway
[d] PSYCHdissemination – International Institute for the Dissemination of Research in Psychology, Córdoba, Spain
[e] Department of Pediatrics, Sørlandet Hospital, Arendal, Norway
[f] Regional Centre for Child and Youth Mental Health and Child Welfare, Department of Mental Health, Norwegian University of Science and Technology, Trondheim, Norway
[g] Maternity ward, St. Olav University Hospital, Trondheim, Norway
[h] Department of Neuroscience, Faculty of Medicine and Health Sciences, Norwegian University of Science and Technology, Trondheim, Norway
[i] Department of Public Health and General Practice, Norwegian University of Science and Technology, Trondheim, Norway
[j] Athinoula A. Martinos Center for Biomedical Imaging, Department of Radiology, Massachusetts General Hospital, United States

A B S T R A C T

Development of the cerebral cortex may be affected by aberrant white matter development. Preterm birth with very low birth weight (VLBW) has been associated with reduced fractional anisotropy of white matter and changes in cortical thickness and surface area. We use a new methodological approach to combine white and gray matter data and test the hypothesis that white matter injury is primary, and acts as a mediating factor for concomitant gray matter aberrations, in the developing VLBW brain. T1 and dMRI data were obtained from 47 young adults born preterm with VLBW and 73 term-born peers (mean age = 26). Cortical thickness was measured across the cortical mantle and compared between the groups, using the FreeSurfer software suite. White matter pathways were reconstructed with the TRACULA software and projected to their cortical end regions, where cortical thickness was averaged. In the VLBW group, cortical thickness was increased in anteromedial frontal, orbitofrontal, and occipital regions, and fractional anisotropy (FA) was reduced in frontal lobe pathways, indicating compromised white matter integrity. Statistical mediation analyses demonstrated that increased cortical thickness in the frontal regions was mediated by reduced FA in the corpus callosum forceps minor, consistent with the notion that white matter injury can disrupt frontal lobe cortical development. Combining statistical mediation analysis with pathway projection onto the cortical surface offers a powerful novel tool to investigate how cortical regions are differentially affected by white matter injury.

1. Introduction

Cerebral white matter injury is considered the dominant lesion in children born preterm with very low birthweight (VLBW; < 1500g) (Volpe, 2008). White matter axons grow rapidly during the last trimester of gestation and in the early postnatal period, the peak period of vulnerability for periventricular leukomalacia (PVL). The main initiating pathogenic mechanisms in PVL are ischemia and inflammation, triggered by such conditions as maternal intrauterine infection or postnatal sepsis (Volpe, 2009). The resulting widespread gliosis and axonal damage may also disturb the early formation, development, and maturation of the cerebral cortex (Back, 2014; Back and Miller, 2014; van Tilborg et al., 2016; Volpe, 2009). Neurons migrate from the subventricular zone to their cortical destination during the second trimester of gestation (Rakic, 1988; Sidman and Rakic, 1973) and disruption of this process or of subsequent synapse formation, pruning or myelination can lead to cortical maldevelopment. Although both white matter and gray matter structural abnormalities are detectable using quantitative magnetic resonance imaging (MRI), little is known regarding the relationship between white matter injury and cortical dysmaturation or

* Corresponding author. Center for Early Brain Development, Department of Clinical & Molecular Medicine, Norwegian University of Science and Technology, 7489, Trondheim, Norway.
E-mail address: lars.rimol@ntnu.no (L.M. Rimol).

https://doi.org/10.1016/j.neuroimage.2018.11.050
Received 12 September 2018; Received in revised form 14 November 2018; Accepted 27 November 2018
Available online 28 November 2018

maldevelopment.

Diffusion-weighted MRI (dMRI) has revealed that diffuse white matter injury is often accompanied by low fractional anisotropy (FA), which can be indicative of disorganization or decreased microstructural integrity, and decreased FA values are therefore considered a pathophysiological feature of diffuse white matter injury (van Tilborg et al., 2016). dMRI studies have demonstrated reduced FA in preterm born children at term equivalent age, compared to term born controls (Huppi et al., 2001). These changes appear to persist through childhood and into adolescence (Anjari et al., 2007; Bassi et al., 2008; Constable et al., 2008; Nagy et al., 2003; Partridge et al., 2004; Rose et al., 2008; Vangberg et al., 2006; Yung et al., 2007) and early adulthood (Eikenes et al., 2011; Olsen et al., 2018). However, tractography studies also find increased FA in several white matter pathways in children and teenagers born preterm (Groeschel et al., 2014; Travis et al., 2015), possibly reflecting selective disruption of one fiber population in crossing fiber regions.

A number of brain morphometry studies have demonstrated cortical thinning in posterior temporal and parietal regions, and cortical thickening in frontal and occipital regions, in preterm born children (Sølsnes et al., 2015a), adolescents (Martinussen et al., 2005), and young adults (Bjuland et al., 2013; Nam et al., 2015). The source of this discrepancy is unknown but it is possible that temporo-parietal reductions can be explained, at least partly, by axonal degeneration due to focal PVL, whereas the increases in frontal thickness may reflect disrupted or delayed pruning, dysmyelination, and/or other diffuse white matter damage.

The main purpose of this study was to test the hypothesis that cortical maldevelopment is secondary to primary white matter injury. The precise relationship between white matter injury and cortical deviations in VLBW is largely uncharted territory and difficult to test directly in an observational study. However, if the hypothesis is correct, and provided that white matter injury manifests as reduced FA, it should be possible to show that FA acts as a statistical mediator on cortical thickness deviations in the VLBW population.

We examined a cohort of 26-year-olds born preterm with VLBW and a coetaneous term-born control group, using surface-based cortical morphometry and dMRI-based tractography (TRACULA). TRACULA reconstructs white matter pathways using information on their relative positions with respect to the surrounding anatomical regions in native space. We projected the endpoints of these white matter pathways onto the subject's cortical surface, thus obtaining cortical regions tailored to the individual's own pathways, and measured cortical thickness in these “endpoint regions.” We then employed statistical mediation analysis (MacKinnon and Dwyer, 1993; Valeri and Vanderweele, 2013) to investigate whether there is an indirect effect of being born with VLBW on cortical thickness, mediated by reduced FA in white matter tracts projecting to the cortical endpoint regions.

First, we investigated group differences in cortical thickness between VLBW and controls, hypothesizing (1) that we would replicate previous findings of increased frontal and occipital, as well as reduced temporo-parietal, cortical thickness (Bjuland et al., 2013; Martinussen et al., 2005; Nam et al., 2015; Sølsnes et al., 2015a). Next, we investigated group differences in FA, anticipating (2) abnormal FA in white matter pathways projecting to cortical regions showing deviant cortical thickness in VLBW (reduction or increase). Third, we hypothesized (3) that deviations of cortical thickness in VLBW are mediated by abnormal FA in the white matter pathways selected in (2).

2. Methods

2.1. Subjects

This is a hospital-based follow-up study of three year cohorts (birth years 1986-88) of subjects born preterm with VLBW (birth weight ≤1500 g) and a term-born control group with normal birth weight (birth weight ≥10th percentile), at around 26 years of age. Detailed inclusion criteria and results from multidisciplinary clinical assessments and cerebral MRI at ages 15 and 20 are reported in earlier publications (Bjuland et al., 2013; Indredavik et al., 2004; Martinussen et al., 2005; Skranes et al., 2007, 2013).

2.1.1. VLBW group

Between 1986 and 1988, 121 VLBW children were admitted to the Neonatal Intensive Care Unit at the St. Olav's Hospital, Trondheim University Hospital, Norway. Of these, 33 died, two were excluded at birth due to congenital syndromes or malformation, and two were excluded at follow-up due to severe cerebral palsy (quadriplegia with mental retardation). Hence, 84 were eligible and invited to participate at 26 years of age, of whom 47 (43% males) consented to participate and had usable MRI data. Two VLBW participants had mild cerebral palsy, classified as grade I-II (both diplegic) according to the Gross Motor Function Classification System (GMFCS).

2.1.2. Term-born control group

The control participants were recruited in Trondheim as part of a multi-center study, in which 1200 pregnant women with a singleton pregnancy and expecting their second or third child, were enrolled before week 20 of pregnancy. A 10% random sample selected by the sealed envelope method was chosen for follow-up, serving as a population reference. The control group comprised 120 children born at term with birth weight ≥10th percentile, adjusted for GA and gender, but since two children were excluded due to congenital malformations, 118 children were eligible for follow up. At 26 years of age, 73 (55% males) individuals consented to participate in MRI scanning and had usable MRI data.

2.1.3. Non-participants

Thirty-seven VLBW and 45 controls were lost to follow-up. Separate independent-samples t-tests for VLBW and controls were conducted to compare birth weight (BW), gestational age (GA), and socio-economic status between participants in the present study and non-participants lost to follow-up. Mean GA was lower for non-participants than participants, both in the VLBW group ($M = 27.9$, $SD = 2.6$ vs. $M = 29.5$, $SD = 2.4$) ($t(82) = 2.98$, $p = .004$) and the control group ($M = 39.4$, $SD = 1.2$ vs. $M = 39.9$, $SD = 1.2$) ($t(116) = 2.43$, $p = .02$). Mean BW was lower for non-participants born with VLBW ($M = 1240$, $SD = 228$ vs. $M = 1084$, $SD = 229$) ($t(82) = 3.10$, $p = .003$) (see Table S2 in Supplementary material for more details). (Table S3 in Supplementary material details clinical and demographic data for those who were excluded due to low MR image quality).

2.1.4. Perinatal data

BW, GA, and perinatal risk factors, such as number of days on mechanical ventilator, total days of stay in the neonatal intensive care unit (NICU) and presence or absence of focal brain pathology seen on neonatal ultrasonography, were recorded.

2.1.5. Cognitive assessment

Intelligence Quotient (IQ) scores were obtained from the Wechsler Adult Intelligence Scale (WAIS) 3rd ed (Wechsler et al., 2003) when the participants were 20 years old, administered by a clinical neuropsychologist (Løhaugen et al., 2010). The full IQ score was based on the results from 11 subtests.

2.1.6. Socio-economic status

Hollingshead's Two Factor index of Social position was used to calculate socio-economic status (SES) based on the education and occupation (adapted to today's categories) of one parent, or the mean index of both parents (Hollingshead, 1957). Parental SES was collected at 14–15 years of age (Indredavik et al., 2004) and supplemented at 19–20 years (Løhaugen et al., 2010).

2.2. MR imaging

2.2.1. Image acquisition

MRI scanning was performed on a 3 T Siemens Skyra scanner, equipped with a quadrature head coil. Two sagittal T1-weighted magnetization prepared rapid gradient echo (MPRAGE) scans were acquired (echo time = 3.45 ms, repetition time = 2730 ms, inversion time = 1000 ms, flip angle = 7°; field of view = 256 mm, voxel size = $1 \times 1 \times 1.33\ mm^3$, acquisition matrix 256×192 x 128, reconstructed to 256×256 x 128). The DTI sequence was a single-shot balanced-echo EPI sequence acquired in 30 non-collinear directions, using the following parameters: TR = 8800 ms, TE = 95 ms, FOV 192×192 mm, slice thickness 2.5 mm, acquisition matrix 96×96. Sixty axial slices were acquired without gap, giving full brain coverage. For each slice, four images without diffusion weighting (b = 0), and 60 images with diffusion gradients were acquired, consisting of 30 images with b = 1000 s/mm^2 and 30 with b = 2000 s/mm^2.

2.2.2. Image analysis

2.2.2.1. Brain morphometry. Cortical reconstruction and subcortical segmentation were performed with the FreeSurfer image analysis suite, version 5.3.0 (https://surfer.nmr.mgh.harvard.edu/). The technical details of cortical reconstruction with FreeSurfer are described elsewhere (Dale et al., 1999; Dale and Sereno, 1993; Fischl and Dale, 2000; Fischl et al., 1999a, 1999b, 2001, 2004b). Matching of cortical geometry across subjects is achieved by registration to a spherical atlas based on individual cortical folding patterns (Fischl et al., 1999b). Cortical thickness estimates were obtained as described in previous publications (Fischl and Dale, 2000; Winkler et al., 2017). The two cerebral hemispheres were processed separately, and cortical thickness was measured in more than 160 000 locations (vertices) across the cortical mantle. The thickness maps were smoothed with a full-width-half-maximum Gaussian kernel of 30 mm (662 iterations).

2.2.2.2. dMRI tractography. TRACULA (TRActs Constrained by UnderLying Anatomy), as implemented in FreeSurfer 5.3.0, was used for dMRI analysis and tractography (Yendiki et al., 2011). Briefly, TRACULA performs global probabilistic tractography with anatomical priors, given a subject's dMRI data and cortical and subcortical segmentation labels from FreeSurfer (Fischl et al., 2002, 2004a, 2004b). TRACULA estimates the posterior probability of each pathway, which consists of a likelihood term that fits the pathway to the diffusion orientations obtained from a "ball-and-stick" model of diffusion (Behrens et al., 2007), as well as a prior term, which incorporates anatomical knowledge on the pathways from a set of healthy adult training subjects. The prior term expresses the probability of each pathway to pass through, or lie adjacent to, each anatomical segmentation label, calculated separately for every point along the pathway's trajectory. The anatomical segmentation labels come from the cortical parcellation and subcortical segmentation of T1-weighted MPRAGE images in FreeSurfer. Thus, the information that TRACULA learns from the training data is only the relative position of the pathway with respect to its surrounding anatomy, and not the absolute coordinates of the pathway in a template space. As a result, it does not require exact alignment of subjects in template space.

In order to test hypothesis (3) that white matter lesions mediate the effect of being born preterm with VLBW on cortical thickness, we selected the white matter pathways that project to cortical regions where abnormal cortical thickness has been observed in VLBW. Increased cortical thickness has consistently been observed in the orbitofrontal and medial anterior superior frontal gyrus (SFG) and the medial occipital lobe, and reduced cortical thickness in temporo-parietal regions bilaterally (Bjuland et al., 2013; Nam et al., 2015; Rimol et al., 2016; Sølsnes et al., 2015a). Therefore, based on these previous cortical thickness findings, the following eight pathways were included: corpus callosum forceps minor (projects to: anterior medial SFG), uncinate fasciculus left and right (from anterior temporal to orbitofrontal cortex), corpus callosum forceps major (to medial occipital cortex), superior longitudinal fasciculus – parietal bundle (SLF(p) left and right, superior longitudinal fasciculus–temporal bundle (SLF(t), also called arcuate fasciculus) left and right (all of which project from the frontal lobe to the temporo-parietal junction). Mean fractional anisotropy (FA), mean diffusivity (MD), radial diffusivity (RD), and axial diffusivity (AD) were assessed in each of the eight selected white matter pathways. For each pathway, only subjects that passed a tractography quality control were included in the analyses.

2.2.2.3. Tract endpoint cortical thickness analysis. In order test the hypothesis that cortical thickness changes are secondary to FA reductions in white matter tracts, we projected the endpoints of the various tracts onto the cortical surface in the subject's native space and obtained cortical thickness data from these cortical endpoint regions. Thus, we obtained regions of interest for the endings of each pathway on the cortical surface by mapping the probability distribution of each of the two end regions of each pathway, as computed by TRACULA, from its native dMRI space to the space of the same subject's T1-weighted image. We projected the tract endpoints onto the gray/white matter surface by sampling along the surface normal vector, anywhere within 6 mm (3 dMRI-space voxels) of the gray/white junction, and then smoothing along the surface with a 2D Gaussian kernel of 6 mm full width at half maximum. The advantage of this approach is that instead of relying on regions defined on an average brain, which would require highly accurate inter-subject registration, TRACULA reconstructs white matter pathways using only prior information on the relative positions of the pathways with respect to the surrounding anatomical regions in native space.

2.2.2.4. Tractography pointwise analysis. In order to explore how the significant group effects were distributed along the selected white matter pathways, data were obtained from multiple contiguous cross-sections along each pathway. TRACULA estimates the posterior probability distribution of each pathway in the native dMRI space of each subject and finds the maximum probability path, which is a 1D curve in that space. It then calculates the expected value of FA, MD, RD, or AD as a function of position along the pathway by performing a weighted average of the values of each of these four measures at each cross-section of the pathway. These cross-sections are defined at each voxel along the maximum probability path. This yields a 1D sequence of values for each of the four measures, computed in the native space of each subject. Correspondence of points between these sequences from different subjects is established by aligning the mid-points of the sequences. These sequences can be used for pointwise analyses of each measure along the trajectory of a pathway.

2.3. Statistics

2.3.1. Statistical software

Demographic and clinical variables were examined with IBM SPSS 20. Student's t-test was used for group comparisons of demographic and clinical characteristics, and the Chi square test was used to compare the sex distributions of the groups. The software package 2015b (The MathWorks, Inc., Natick, Massachusetts, United States) was used for statistical analysis of brain morphometry data.

2.3.2. Cortical morphometry

General Linear Models (GLM), with cortical thickness as dependent variable, and age (at time of MR scan) as a continuous predictor, and sex and group (controls, VLBW) as categorical predictors were fitted for every vertex across the cortex. Interactions between age and group, and sex and group, were tested for across the cortical mantle and no

significant interaction was found in any analysis (corrected with 5% FDR), so interaction terms were not included in the final analyses. Finally, significance tests were performed to compare the VLBW group to the group of term-born controls. The hemispheres were analyzed separately and maps of effect sizes and p-values (p-maps) were generated. To correct for multiple comparisons, the two p-maps from left and right hemisphere were combined and thresholded to yield an expected false discovery rate (FDR) of 5% across the hemispheres (Benjamini et al., 2006).

2.3.3. Analysis of dMRI-data

The dMRI-data from TRACULA were analyzed using GLMs with mean FA, MD, RD, or AD as dependent variable, age (at time of MR scan) and the total (head) motion index (TMI) from Yendiki et al. (2013) as continuous predictors, and sex and group (controls, VLBW) as categorical predictors. Interactions between group and age, sex, and TMI were tested for and not found to be significant for any of the pathways studied. However, there were non-significant trends for some of the pathways toward a negative relationship between TMI and FA in the VLBW group. Closer analysis revealed that this was limited to two subscales of TMI representing signal dropout, i.e. "Percentage of slices with signal drop-out" and "Signal drop-out severity" (Yendiki et al., 2013). In order to control for any undue influence from low quality data on our analyses, we reran all dMRI analyses excluding subjects that had a Z-score >2 on either of the two signal dropout scores. After the outliers had been removed, there were no significant or trend-level interactions between group and TMI on FA. The main conclusions remained the same in both analyses, regardless of whether the outliers were included or excluded. The results from the analyses without outliers are presented in the paper. Contrast vectors were specified to test for group differences and the Holm-Bonferroni procedure was used to correct for multiple comparisons across the eight pathways that were considered.

2.3.4. Mediation analysis: combining cortical thickness and dMRI

To test the hypothesis that group differences in gray matter (cortical thickness) are secondary to white matter injury, we performed a statistical mediation analysis that assesses indirect effects of the independent variable (group) on the dependent variable (cortical thickness) through the independent variable's effect on a mediating variable (FA) (MacKinnon and Dwyer, 1993; Valeri and Vanderweele, 2013). We used cortical thickness data from the cortical endpoint regions of each pathway (see Fig. 3) as the exposure variable, and fitted two models; one with FA as dependent variable and group (controls = 0, VLBW = 1), sex and age as predictor variables, and a second model with cortical thickness as dependent variable and group, sex, age, FA, and group*FA as predictor variables. The natural direct effect (NDE) and natural indirect (NIE) effect of group (VLBW) on cortical thickness were calculated as described in Valeri and Vanderweele (2013). The NDE expresses how large the difference in cortical thickness would be between VLBW (exposure = 1) and controls (exposure = 0) if, for each participant, the mediator (FA) were kept at the mean level of the control group. The NIE expresses how much cortical thickness would change, on average, if exposure were kept at 1 (VLBW) but the mediator were changed from the level it would take if exposure = 0 to the level it would take if exposure = 1. The sum of NDE and NIE comprises the total effect of the exposure variable (VLBW) on the dependent variable (cortical thickness), and the NIE represents the mediation effect of FA in the current analyses. For each cortical endpoint region, NDE and NIE were calculated using the average values for age and sex from the entire sample. The software Mplus 8 (Muthén and Muthén, 1998–2011) was used to bootstrap confidence intervals for NDE and NIE.

2.3.5. Tractography pointwise analysis

To explore the localization of group differences in FA along the pathway, pointwise significance tests were performed for each 2.5 mm segment. GLMs were fitted for each segment, with FA as dependent variable and group, sex, age, and TMI as predictors, and group differences were tested for significance. In order to control the false positive rate, we chose to report findings only if they showed a significant group difference ($p < .05$) over a contiguous segment of at least 1 cm in length along a given pathway.

2.4. Ethics

The Regional Committee for Medical Research Ethics (Norwegian Health Region IV) approved the study protocols (project numbers: 78–00 May 2000; 4.2005.2605; 2013/636 REK midt), and every participant gave written informed consent.

3. Results

3.1. Demographic and clinical variables

Demographic and clinical variables are presented in Table 1. There was a statistically significant ($p < .05$) difference in IQ between the VLBW group ($M = 89$, $SD = 13.0$) and the control group ($M = 102$, $SD = 12.7$); $t_{89} = 4.73$, $p = 8*10^{-6}$. Only three participants (out of 25 (12%) for whom neonatal ultrasound data were available) had grade 1 intraventricular hemorrhage (IVH) (see Table 1).

3.2. Cortical morphometry

Fig. 1 displays cortical regions where VLBW showed either significantly reduced (red-yellow) or increased (blue) cortical thickness compared to term-born controls. Cortical thickness was reduced bilaterally in lateral temporo-parietal regions and was increased mainly on the medial aspect of the hemispheres, primarily in the orbitofrontal cortex (OFC), extending into the rostral medial superior frontal gyrus (SFG), but also in the medial occipital lobe, including the cuneus.

3.3. Analysis of dMRI-data

Table 2 shows mean FA, AD, RD, and MD from the whole tract, for the eight tracts investigated. The statistical analyses showed significantly reduced FA in the VLBW group, relative to term-born controls, in forceps

Table 1
Demographic, clinical, and cognitive data for VLBW and term-born controls at 26 years of age**.

	n	VLBW	n	Controls	*p*-Value£
Birth weight*	47	1240 (550–1500)	73	3704 (2670–5140)	–
Gestational age*	47	29.5 (25.0–35.0)	73	39.9 (37.0–43.0)	–
Socio-economic status†	41	3.4 (3.0–3.8)	62	3.9 (3.6–4.1)	.09
IQ£	36	89 (13.0)	56	102 (12.6)	<.0001
Age at scan†	47	26.3 (25.2–28.4)	73	26.4 (25.6–27.3)	–
Sex (#males/#females)	47	27/20		73	33/40
Days in NICU§	46	57 (23–386)			
Days on ventilator§	46	1 (0–35)			
Intra ventricular hemorrhage¤					
• #grade 0 or 1 (#grade 1)	25 (3)				
• #grade 2,3, or 4	0				

** IQ measured at age 20.
Data given as means with either * = range, † = 95% CI, or £ = standard deviation; or as § = median (range).
£Student t-test: VLBW vs controls.
¤ IVH data were available for 25 out of 47 individuals born with VLBW.
Abbreviations: VLBW: very low birth weight; CI: confidence interval.

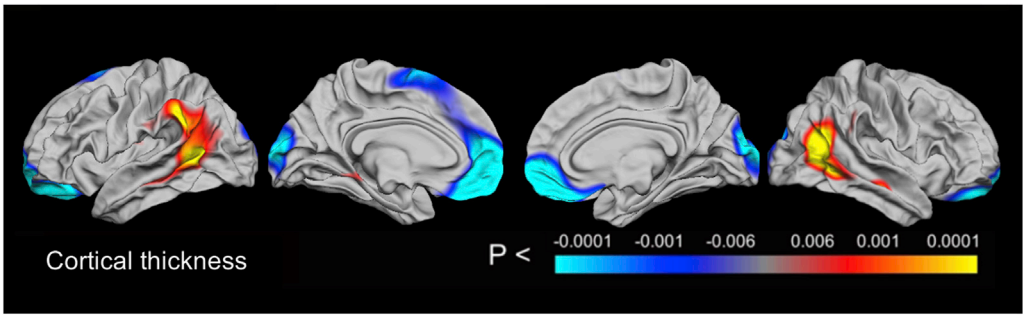

Fig. 1. Group differences in cortical thickness.
The figure shows p-value maps from significance tests of group differences in cortical thickness, corrected with a 5% false discovery rate. Red to yellow regions show significant reduction in the VLBW group relative to the term-born control group. Blue to light blue regions show significant cortical thickening in the VLBW group relative to the controls.

Table 2
Mean FA, AD, RD, and MD, by group (raw data).

White matter pathway	FA		AD		RD		MD	
	Controls	VLBW	Controls	VLBW	Controls	VLBW	Controls	VLBW
Forceps major	0.626	0.613	0.001292	0.001283	0.000377	0.000389	0.000682	0.000687
Forceps minor	0.572	0.554	0.001150	0.001124	0.000397	0.000408	0.000648	0.000646
Left SLF(p)	0.424	0.441	0.000862	0.000873	0.000442	0.000429	0.000582	0.000577
Right SLF(p)	0.465	0.474	0.000923	0.000939	0.000435	0.000433	0.000597	0.000602
Left SLF(t)	0.426	0.450	0.000872	0.000893	0.000438	0.000423	0.000582	0.000580
Right SLF(t)	0.447	0.467	0.000902	0.000930	0.000430	0.000423	0.000588	0.000592
Left UNC	0.448	0.422	0.001047	0.001044	0.000499	0.000525	0.000681	0.000698
Right UNC	0.444	0.424	0.001032	0.001028	0.000495	0.000513	0.000674	0.000685

Abbreviations: VLBW: very low birth weight; FA: Fractional anisotropy, AD: Axial diffusivity, RD: Radial diffusivity, MD: Medial diffusivity.
SLF(p/t): Superior longitudinal fasciculus (parietal/temporal part), UNC: uncinate fasciculus.

minor and left and right uncinate fasciculus, as well as increased FA in the right SLF(p) (Table 3). In order to explore the possible causes of reduced FA, the AD (greatest eigenvalue of the diffusion tensor) and RD (average of the two smallest eigenvalues of the diffusion tensor) were analyzed. Left and right uncinate fasciculus showed significantly increased RD, and right SLF(t) showed significantly increased AD. There were trend-level increases in AD in right SLF(p) and left SLF(t), and a trend-level decrease in AD and increase in RD in forceps minor. In addition, MD was significantly increased in the left uncinate.

3.4. *To what extent do FA reductions in white matter mediate the effect of VLBW on cortical thickness?*

Table 4 shows mean cortical thickness in the cortical endpoint regions included in the statistical mediation analyses. Table 5 displays the results of the mediation analyses for selected cortical endpoint regions (Supplementary table 1 shows the results for all regions). The results demonstrate significant mediation effects (NIE) for forceps minor bilaterally in the anterior medial SFG and the orbitofrontal cortex. The estimated NIE of VLBW was 13% (of the total effect of VLBW) in the left hemisphere and 22% in the right hemisphere. In other words, FA changes mediated 13% of the cortical thickness increase ascribed to VLBW in the left hemisphere, and 22% in the right hemisphere.

3.5. *Pointwise analyses of dMRI measures along each tract*

The pointwise analyses of group differences showed significantly lower FA in the VLBW group in a 3 cm long segment in the central and frontal lobe portion of the right uncinate fasciculus, as well as a 1 cm long segment in the temporal lobe portion (see Fig. 2). There was also significantly reduced FA in a 4 cm long segment the left uncinate fasciculus. Finally, a 2.25 cm long segment in the central portion of forceps minor and two segments in forceps major, 1 cm on the left and 2.5 cm on the right, also showed reduced FA in the VLBW group.

In order to explain the increased mean FA in the right SLF in the VLBW group, we explored the corticospinal tract, which contains descending projection fibers that cross the association fibers of the SLF in the corona radiata/centrum semiovale region, since crossing fibers are

Table 3
Group differences in FA, AD, RD, MD.

White matter pathway	FA		AD		RD		MD	
	Cohen's d	*p*	Cohen's d	*p*	Cohen's d	*p*	Cohen's d	*p*
Forceps major	-.18	.38	-.16	.46	.24	.25	.06	.78
Forceps minor	-.59	**.005***	-.46	**.027**	.33	.11	-.09	.67
Left SLF(p)	.48	.022	.23	.26	-.45	**.029**	-.21	.30
Right SLF(p)	.61	**.004***	.46	**.026**	-.42	**.04**	.1	.63
Left SLF(t)	.31	.15	.31	.15	-.14	.51	.04	.83
Right SLF(t)	.59	.072	.60	**.006***	-.27	.21	.07	.76
Left UNC	-.92	**.0007***	.03	.91	.92	**.0008***	.71	**.009**
Right UNC	-.68	**.002***	-.09	.69	.57	**.01**	.37	.09

The table shows group differences (VLBW, controls), for the four DTI-parameters considered. The results are from analyses using general linear models with FA, AD, RD, or MD as dependent variable and group, sex, age, and *total motion index* as independent variables. Significant p-values in BOLD; * significant after Bonferroni-Holms correction for multiple comparisons.
Abbreviations: FA: fractional anisotropy, AD: axial diffusivity, RD: radial diffusivity, MD: mean diffusivity.

Table 4
Mean cortical thickness (mm) in cortical endpoint regions corresponding to selected white matter pathways (raw data).

White matter pathway	Controls		VLBW	
	left	right	left	right
Forceps major	2.00	1.96	2.05	2.03
Forceps minor	2.64	2.55	2.77	2.64
SLF (parietal)	2.58	2.55	2.52	2.50
SLF (temporal)	2.75	2.81	2.71	2.77
UNCINATE	2.70	2.58	2.80	2.71

Abbreviations: VLBW: very low birth weight; SLF: Superior longitudinal fasciculus, UNCINATE: uncinate fasciculus.
The table shows the raw averages from each endpoint region; differences in group averages in the table reflect group differences in corresponding cortical regions displayed in the cortical thickness maps in Fig. 1. Forceps minor and uncinate fasciculus project to frontal cortex (orbitofrontal and anteromedial superior frontal gyrus); forceps major projects to the medial occipital and parietal cortex (medial occipital gyrus, cuneus, and precuneus); the superior longitudinal fasciculus projects from the frontal lobe to the temporo-parietal junction.

Table 5
Mediator analysis: To what extent are cortical thickness group differences mediated by reduced FA?

Cortical endpoint region	Direct effect of VLBW (NDE)		Indirect effect of VLBW (NIE)		Total effect of VLBW
	Estimate	95% CI	Estimate	95%CI	
Forceps major, left	.063	(.009, .114)	-.001	(-.015, .004)	.062
Forceps major, right	.081	(.030, .131)	-.002	(-.017, .002)	.079
Forceps minor, left	.122	(.056, .192)	**.018***	**(.002, .050)**	.140
Forceps minor, right	.081	(-.024, .143)	**.023***	**(.002, .058)**	.104
left SLF(p), posterior	-.072	(-.121, −.022)	.00	(-.026, .013)	-.072
right SLF(p), posterior	-.068	(-.125, −.016)	-.007	(-.035, .021)	-.075
left SLF(t), posterior	-.024	(-.082, .031)	.002	(-.012, .025)	-.022
right SLF(t), posterior	-.055	(-.113, .008)	-.017	(-.057, .010)	-.072
left UNC, frontal	.026	(-.049, .102)	.015	(-.056, .101)	.129
right UNC, frontal	.089	(.019, .159)	.026	(-.004, .071)	.115

The table shows the natural direct (NDE) and indirect (NIE) effects on cortical thickness, of being born preterm with VLBW. The total effect of VLBW on cortical thickness is the sum of NDE and NIE. A positive total effect means that VLBW has thicker cortex than the control group. The NIE is the effect of VLBW on cortical thickness that is mediated by FA; * indicates statistically significant estimate of NIE. Bold NIE confidence intervals indicate significant mediation at the 0.05 level. For the association tracts, i.e., SLF(p) and SLF(t), only the posterior endpoint and for uncinate fasciculus, only the frontal lobe cortical endpoint regions are shown, for simplicity. The full table is shown in Supplementary results.
Abbreviations: FA: fractional anisotropy; SLF(p/t): superior longitudinal fasciculus (parietal/temporal part), UNC: uncinate fasciculus; VLBW: Very Low Birth Weight.

known to cause problems for the tensor model and may produce unexpected findings of increased FA (Groeschel et al., 2014). The pointwise analysis revealed that FA was lower in the corona radiata/centrum semiovale region of both pathways in both groups, and that the FA group difference was also located in this region of crossing fibers (see Supplementary figure S1). Hence, it is possible that the FA group difference simply reflects fewer crossing fibers in VLBW.

4. Discussion

We found increased cortical thickness in frontal and occipital regions, as well as reductions in the temporo-parietal junction, in the VLBW group, which is consistent with previous reports on younger cohorts (Bjuland et al., 2013; Martinussen et al., 2005; Nam et al., 2015; Sølsnes et al., 2015a). We found reduced FA in the VLBW group in the left and right uncinate fascicles and the forceps minor, which project to the frontal regions that show increased cortical thickness in VLBW. Finally, we present novel evidence that reduced fractional anisotropy (FA) in forceps minor mediates cortical thickening in the medial superior frontal gyrus (SFG) and the orbitofrontal cortex (OFC), in adults born preterm with VLBW. In the left hemisphere 13%, and in the right hemisphere 22%, of the effect on cortical thickness of being born preterm with VLBW, was mediated by reduced FA in forceps minor. Although this is an observational study, and as such does not prove biological causation, these findings are consistent with the hypothesis that cortical development is affected by white matter injury in VLBW (see **4.7 Limitations** for a discussion of causal inferences).

4.1. Underlying cellular mechanisms

Cortical thickness was reduced in the temporo-parietal junction (inferior parietal gyrus, posterior lateral temporal lobe, supramarginal gyrus), where gray matter structures are vulnerable to the effects of periventricular leukomalacia (PVL) (Pierson et al., 2007), either present as focal gliotic lesions (with or without cysts) or as more diffuse white matter damage. We do not have high-quality neonatal imaging data on focal (cystic and non-cystic) pathology, as no neonatal MRI was available and ultrasonography was typically used only within the first days after birth in the late 1980s. This is not optimal for detecting focal PVL, which tends to evolve during the first 2–3 weeks after birth. It was not possible to diagnose diffuse PVL with the ultrasound equipment used in the NICU at the time.

The literature suggests that axonal injury and neuronal loss are associated with significant necrotic white matter damage, as results from focal cystic PVL (Back and Miller, 2014). This is consistent with a reduction in FA, as observed in the forceps minor in this study, together with reduced AD - a marker of axonal injury (Song et al., 2003). The underlying mechanism for neuronal loss appears to be axonal degeneration, with retrograde and anterograde (Wallerian, trans-synaptic) effects leading to secondary gray matter degeneration in the overlying cortex (Back, 2014; Volpe, 2009). In addition, the preterm brain is enriched with immature neurons that do not degenerate in response to ischemia (Dean et al., 2013) but nevertheless display disturbances in maturation of dendritic arbors and synapse formation in the cortex (Back, 2014). There is evidence that although mild or moderate hypoxia-ischemia rarely leads to neuronal loss, it may ultimately affect the development of cerebral networks and lead to reduced connectivity (Dean et al., 2014). Severe focal PVL is less common in modern cohorts (Buser et al., 2012; Hamrick et al., 2004) but not unlikely in our cohort from the 1980ies. Thus, it is possible that the bilateral cortical thickness reductions in the temporo-parietal junction seen in this study can be explained by a combination of undiagnosed focal PVL, with concomitant neuronal degeneration, and primary cortical dysmaturation caused by prenatal oxidative stress.

The present findings suggest most of the effect of VLBW on cortical thickness in the frontal lobe is independent of white matter injury. However, one factor in the apparent thickening of the frontal cortex in VLBW may be reduced myelination in white matter tracts located within and near the deepest layers of the cortex. Unmyelinated axons can give a T1 signal similar to gray matter, so it is possible that increased cortical thickness (as it appears on MRI) reflects dys- or demyelination in these pathways (Rimol et al., 2016). Significant group differences in FA were only observed in the middle portions of the pathways but since there was greater across-subjects variability towards the extremes of the pathways

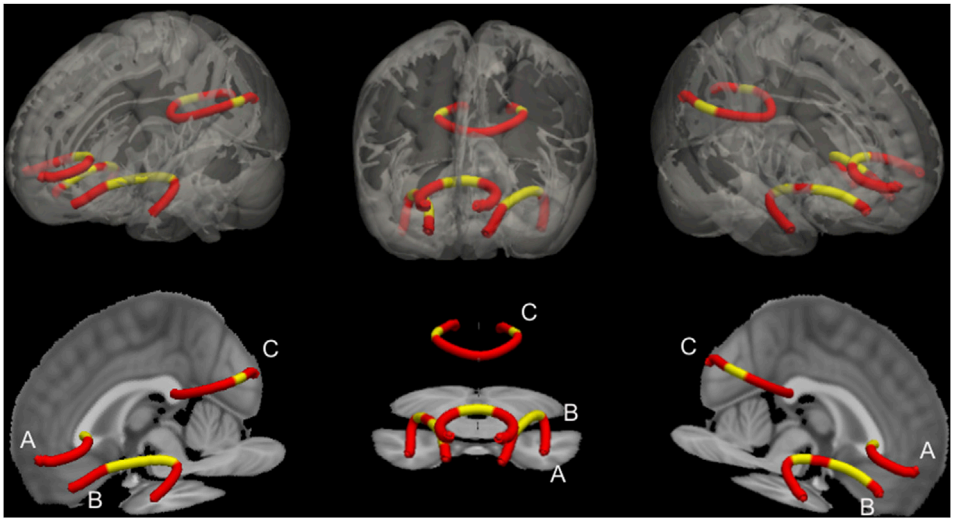

Fig. 2. Pointwise analysis of FA data.
The figure shows significance tests of group differences in FA along left and right uncinate fasciculus (A), forceps minor (B), and forceps major (C). The tracts were divided into 2.5 mm long segments in each subject's native space, and a weighted FA average was obtained from each segment. The p-values are derived from general linear models fitted for each segment along the tract, with FA as dependent variable, group (term-born controls, VLBW) and sex as categorical predictors, and co-varying for age at scan and the total motion index. The false positive rate was controlled by only including findings that show a significant group difference ($p < .05$) over a contiguous segment of at least 1 cm in length. Yellow segments represent significantly reduced FA in VLBW relative to term-born controls.

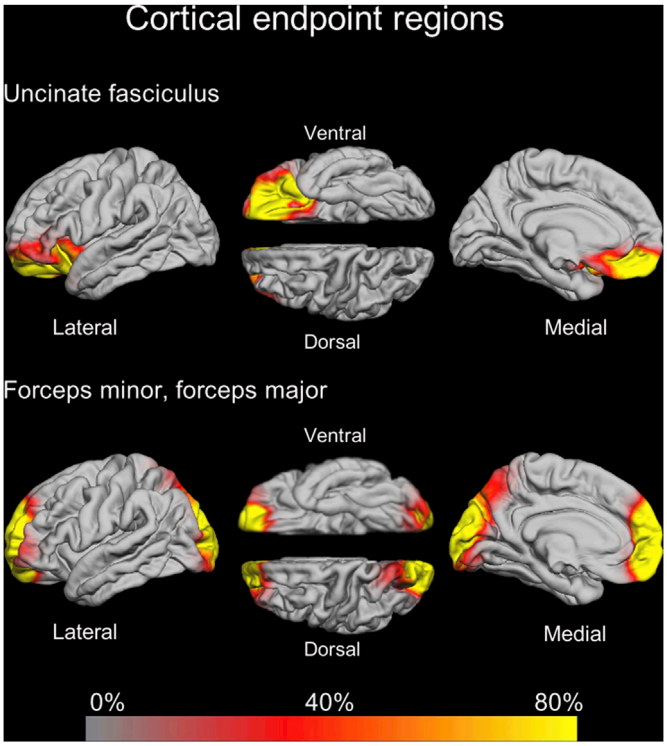

Fig. 3. Cortical endpoint regions.
The figure displays the cortical endpoint regions for left uncinate fasciculus (upper panel), forceps minor and forceps major (bottom panel). The endpoint regions were localized in each subject's native space, and cortical thickness data were extracted from the region. In order to visualize the locations of endpoint regions across subjects, the regions were registered to a common space (*fsaverage* from FreeSurfer). The maps show in what percentage of subjects a given location (vertex) was included in the cortical endpoint region. Thus, red locations were represented in around 40% of endpoint regions, yellow locations in (at least) 80% of endpoint regions.

(see **Limitations**), we cannot rule out similar FA reductions there.

The usual progression of cortical development after childhood is toward cortical thinning due to elimination of synapses ("pruning"). Selective elimination of cortical synapses is a crucial biological process that begins around 7–10 years (Jeon et al., 2015), or with the onset of puberty (Goldman-Rakic et al., 1997), and likely serves to increase efficiency in cognition and behavior (Giedd, 2004). Dendritic elimination is regulated by several neurotrophic factors (Callaway and Borrell, 2011; McAllister et al., 1996) that are believed to act preferentially on active neurons (McAllister et al., 1996). It is possible that dysregulation of trophic factors could affect activity dependent elimination processes, perhaps adversely affected by damage to cortico-cortical connections, leading to arrested pruning and thicker cortex.

Although it may seem unlikely at age 26, we cannot rule out the possibility that pruning is simply delayed in the frontal lobe in our VLBW participants. Despite the widely accepted view that pruning is completed by the end of adolescence (Huttenlocher, 1979), it has recently been demonstrated that elimination of dendritic spines on pyramidal neurons in the dorsolateral prefrontal cortex goes on well into the third decade of life (Petanjek et al., 2011). If this is the case, the observed cortical thickness differences may still to some extent be reversible. Finally, an alternative hypothesis is that damage to long association fibers (as are found in forceps minor) could result in axotomized pyramidal cells being "transformed from long-projective neurons into local-circuit interneurons with an intracortical distribution of their axons" (Marin-Padilla, 1997). This may in turn lead to local neuronal hypertrophy and increased neuropil, contributing to an actual increase in cortical thickness in VLBW. It is unlikely that this can fully explain the mediation effects observed here, but it could be a contributing factor.

4.2. Lack of mediation findings in the occipital lobe

Why did FA act as a statistical mediator for increased cortical thickness in the frontal lobe and not in the occipital lobe? Group differences in cortical thickness were observed in the medial occipital lobes, with increased thickness in the VLBW group, but these were smaller and less extensive than in the frontal lobes. The cortical regions displaying a substantial increase in thickness comprised a smaller proportion of the entire endpoint region for forceps major than was the case for forceps minor, which may explain the lack of statistical mediation effects for forceps major. It is of course also possible that as frontal regions mature later (Oishi et al., 2011), they may be more susceptible to peri- and postnatal insults, including white matter injury, than posterior sensory regions.

4.3. Decreased FA in forceps minor and uncinate fasciculus

We found FA reductions in the VLBW group in the left and right uncinate fascicles and forceps minor, as well as trend-level reductions in forceps major. In general, a decrease in white matter FA may occur because diffusivity parallel to the tract (AD) decreases, diffusivity perpendicular to the tract (RD) increases, or both. The precise cause of

changes in FA is difficult to determine (Boretius et al., 2012) but a general assumption is that AD reduction, as observed in forceps minor in the present study, is related to poor organization of fiber structure and/or axon injury, whereas increased RD, observed in both uncinate fascicles, tends to reflect hypo- or demyelination and/or reduced axonal diameter or density (Oh et al., 2004; Song et al., 2002, 2003). Hypomyelination in VLBW is associated with diffuse PVL, in which the main cellular targets are pre-oligodendrocytes (preOLs) - precursors to the myelinating oligodendrocytes - which are sensitive to hypoxia and abundant in cerebral white matter after term. Damage to preOLs involves "a disrupted cellular response" whereby preOLs fail to differentiate and mature into myelinating oligodendrocytes (Buser et al., 2012). In diffuse white matter damage, necrosis and axonopathy do not appear to contribute substantially to myelination failure.

Low FA values have been associated with adverse long-term outcome in the preterm population (Allin et al., 2011). Multiple studies have reported reduced FA in the corpus callosum of preterm born children and adolescents (Anjari et al., 2007; Counsell et al., 2007, 2008; Vangberg et al., 2006), albeit not specifically in the forceps minor. Reduced FA in uncinate fasciculus has previously been reported in adolescents (Constable et al., 2008; Mullen et al., 2011) and adults (Allin et al., 2011) born very preterm. There is disagreement as to the exact functions of the uncinate fasciculus but there is evidence implicating it in language-related functions, such as auditory working memory (Dick and Tremblay, 2012; Papagno, 2011) and lexical and semantic retrieval (Von Der Heide et al., 2013). Notably, the right uncinate fasciculus has been found to be associated with reading skills in studies of full term children (Travis et al., 2017) and reading skills and verbal IQ in several studies of preterm children (Constable et al., 2008; Feldman et al., 2012; Mullen et al., 2011; Schaeffer et al., 2014; Travis et al., 2017).

Finally, it should be noted that this study was limited to pathways that project to cortical regions showing aberrant cortical thickness in VLBW. Previous studies on the present cohort demonstrated FA reductions in other parts of the corpus callosum, and the fronto-occipital fasciculus/inferior longitudinal fasciculus, using alternative methods of DTI analysis (Eikenes et al., 2011; Skranes et al., 2009; Vangberg et al., 2006).

4.4. Increased FA in the superior longitudinal fasciculus

FA was increased in the right parietal superior longitudinal fasciculus (SLF) in the VLBW group. We have previously shown increased FA in the right SLF in the same cohort at 23 years (Eikenes et al., 2011) and in another Norwegian cohort at nine years (Sølsnes et al., 2015b). Increased FA may reflect decreased numbers of crossing fibers, possibly related to axonal loss, and/or high myelin content in specific pathways. Consistent with reduced branching or crossing, AD was increased bilaterally in the parietal SLF in the VLBW group. RD was increased in the right SLF (temporal and parietal), which may reflect increased myelination, possibly from compensatory processes in the VLBW brain. However, increased myelination appears to be most likely within white matter tracts demonstrating single fiber orientations (De Santis et al., 2014). A detailed analysis of the various segments along the tract, revealed that the FA increase was mainly present in the corona radiata/centrum semiovale region, where especially descending motor fibers cross the association fibers of the longitudinal fasciclus, as well as commissural and other association fibers (see Supplementary figure S1). The interpretation of increased FA is not straightforward in a crossing fiber region (Douaud et al., 2011; Jones, 2010), but it could occur as a result of selective disruption to one of the fiber populations present (Tuch et al., 2005). Hence, the present findings may reflect a reduction in the number or density of crossing fibers, from axonal loss in several white matter pathways in the VLBW group. These findings are to some extent consistent with previous literature; studies of preterm/VLBW cohorts have found conflicting results in the corona radiata/centrum semiovale region, including reduced FA (Anjari et al., 2007; Constable et al., 2008; Huppi et al., 1998, 2001), increased FA (Gimenez et al., 2008; Groeschel et al., 2014; Jurcoane et al., 2016; Rose et al., 2008), and no difference in FA relative to term-born controls (Cheong et al., 2009).

Studies have estimated that the majority of white matter voxels (60–90%) contain crossing fibers (Jeurissen et al., 2013). The TRACULA tractography uses a ball and stick model that accounts for fiber crossings, but the FA values themselves still come from the tensor model and are therefore subject to the usual confounds. Additional neuroimaging techniques may be required to obtain voxel-based estimates for the proportion of crossing fibers and tissue myelination (Abhinav et al., 2014), in order to further our understanding of the neurobiological underpinnings of decreases and increases in FA in the VLBW population (Travis et al., 2015). This may be especially true in regions with a high degree of fiber crossing, where it is particularly challenging to distinguish among the various interpretations for FA.

4.5. The influence of modern NICU treatment

We previously reported increased cortical thickness in frontal regions and decreased thickness in temporo-parietal regions, but few signs of white matter injury, in 9 year-olds born with VLBW in the 2000s (Sølsnes et al., 2015a). We speculated that reduced white matter injury may reflect improved neonatal intensive care (Sølsnes et al., 2015b; Rimol et al., 2016) because white matter development is vulnerable to postnatal morbidity, whereas cortical development may be more likely to be compromised already in utero (Thomason et al., 2017). In general, dMRI studies of the preterm population seem to find more FA reductions in young adults than in adolescents (Eikenes et al., 2011), and there is evidence from animal studies that long-standing activation of microglia can lead to chronic inflammation in white matter that continues to affect myelination long after birth (Wideroe et al., 2011). If this is the case, early white matter injury in VLBW is not only irreversible but has increasing impact over time, involving also late myelinating tracts such as the association tracts projecting to frontal areas (Eikenes et al., 2011). It is therefore possible that frontal lobe white matter injury has not yet reached its maximum impact in younger preterm/VLBW cohorts and may, thus, be harder to detect, particularly in small samples. However, even assuming there is progressive white matter injury in VLBW; it is still unclear how this is related to seemingly static gray matter lesions from late childhood up until the mid-twenties. Studies of white matter and gray matter integrity in younger preterm/VLBW cohorts could provide information on the timing of gray and white matter deviations after preterm birth but, ultimately, longitudinal studies are necessary in order to determine whether the observed group differences seen here and in other studies reflect sustained injuries from birth, or delayed differences that reflect altered maturation (Travis et al., 2015).

4.6. VLBW in a lifespan perspective

Being born preterm with VLBW was associated with thicker cortex in the orbitofrontal gyri and the rostral medial superior frontal gyrus (SFG). These results are similar to previous findings from the same VLBW cohort at age 15 (Rimol et al., 2016) and age 20 (Skranes et al., 2013), as well as an English VLBW cohort of 15 year-olds (Nam et al., 2015). In a recent longitudinal study on the present cohort, we did not find any evidence of a group difference in the developmental trajectories for cortical thickness from 15 to 20 years (Rimol et al., 2016). Taken together, these findings are consistent with static group differences in cortical morphology between VLBW and term-born controls from age 15 to age 26. However, longitudinal image processing and statistical analyses are required to draw firm conclusions about developmental trajectories between 20 and 26 years. Since a higher field strength scanner (3T) was used at 26 years, replacing the 1.5T scanner used in the previous studies at 15 and 20 years, longitudinal analyses were not feasible here.

4.7. Limitations

We demonstrate evidence of statistical mediation by utilizing a novel analytic tool that allows for directly linking each subject's white matter and cortical thickness data with anatomical precision (in native space). For our mediation analyses to be valid, and allow for a causal interpretation of the observed associations, the mediator (FA) cannot be a confounding variable, i.e., it cannot both cause VLBW (the exposure variable) and increased cortical thickness (the outcome) (MacKinnon and Dwyer, 1993). We argue that the direction of causality goes from VLBW to FA, as it is implausible that reduced FA causes preterm birth or VLBW.

It should be noted that VLBW/preterm birth here serves as a proxy for several pre- and postnatal factors that may contribute to deviant adult brain structure. Fetal growth restriction (FGR), which may affect prenatal brain development and lead to VLBW, is likely caused by a range of pathophysiological factors that affect the intrauterine environment and, potentially, prenatal brain development. The most common such factors are poor placental function, causing malnutrition, and hypoxia in utero (McMillen et al., 2001; Pollack and Divon, 1992). Adverse neurodevelopmental effects are, however, not limited to prenatal brain damage. Although preterm birth is usually triggered by prenatal pathology, it is is likely to be the result of a cascade of adverse events that are initiated during pregnancy and continuing at or after birth. For instance, inflammation may lead to placental dysfunction and/or FGR, which may both harm the fetal brain and render it vulnerable to perinatal injury caused by respiratory and circulatory disturbances, insufficient nutrition, the stressors of the NICU environment *et cetera*. This paints a complex picture of unmeasured pre- and peri-/postnatal causal factors which could, in theory, affect both the exposure variable (VLBW) and the mediator (FA), as well as the outcome variable (cortical thickness), and hence act as unmeasured confounders. This could affect the validity of the causal assumptions made in the mediation analysis and thus, by extension, any inferences made about causal mechanisms (Valeri and Vanderweele, 2013). The remedy for unmeasured confounders is to measure them and include them in the statistical analysis. A limitation of this study is the lack of relevant clinical data, such as high quality ultrasound data (to detect fetal growth restriction) and high quality clinical data describing postnatal morbidity, which could help control for various pre- and postnatal causal factors that influence brain growth.

Understanding the relationship between white and gray matter in normative brain development will require neuroimaging in large population studies, which is currently limited. In spite of these limitations, the current method seems promising as a means to investigate the relationship between white and gray matter injury in VLBW, or other clinical populations.

Finally, the pointwise FA analyses visualized in Fig. 2 were based on across-subject alignment from the center of the pathway, without nonlinear volumetric inter-subject registration. Therefore, we are most confident that we are comparing anatomically homologous regions in the central portion of the pathway. Since the length of the pathway differs across individuals, the number of subjects with data is reduced towards the extremes, particularly in the final 1–1.5 cm of the pathway. In addition, across-subject variability typically also increases towards the end of a pathway. Statistical power to detect group differences is therefore reduced there and the risk of committing Type II errors (false negatives) is increased.

5. Conclusions

We confirmed our first hypothesis that cortical thickness is still aberrant in individuals born with VLBW in their late 20ies, including frontal and occipital increases and temporo-paretial decreases in cortical thickness. We also confirmed our second hypothesis that FA is reduced in VLBW, in several white matter pathways projecting to cortical regions with aberrant cortical thickness, indicating compromised white matter integrity. Finally, we confirmed our third hypothesis, demonstrating that cortical thickening in orbitofrontal and anterior frontal brain regions in VLBW is partly mediated by lower FA in the forceps minor of the corpus callosum, which suggests cortical development in these regions is sensitive to white matter injury. The current method, using TRACULA to project white matter tracts onto the cortical surface to measure cortical thickness and employing statistical mediation analysis, appears promising as a means to investigate the relationship between white and gray matter injury in clinical populations.

Acknowledgments

This research was supported by grants from the Research Council of Norway (213732) and the Central Norway Regional Health Authority (46055600-2). This study used Abel, a computer cluster operated and Department for Research Computing at USIT, the University of Oslo IT-department to MRI images in FreeSurfer. Abel is owned by the University of Oslo and the Norwegian metacenter for High Performance Computing (NOTUR).

Appendix A. Supplementary data

Supplementary data to this article can be found online at https://doi.org/10.1016/j.neuroimage.2018.11.050.

References

Abhinav, K., Yeh, F.C., Pathak, S., Suski, V., Lacomis, D., Friedlander, R.M., Fernandez-Miranda, J.C., 2014. Advanced diffusion MRI fiber tracking in neurosurgical and neurodegenerative disorders and neuroanatomical studies: a review. Biochim. Biophys. Acta 1842, 2286–2297.

Allin, M.P., Kontis, D., Walshe, M., Wyatt, J., Barker, G.J., Kanaan, R.A., McGuire, P., Rifkin, L., Murray, R.M., Nosarti, C., 2011. White matter and cognition in adults who were born preterm. PLoS One 6 e24525.

Anjari, M., Srinivasan, L., Allsop, J.M., Hajnal, J.V., Rutherford, M.A., Edwards, A.D., Counsell, S.J., 2007. Diffusion tensor imaging with tract-based spatial statistics reveals local white matter abnormalities in preterm infants. Neuroimage 35, 1021–1027.

Back, S.A., 2014. Cerebral white and gray matter injury in newborns: new insights into pathophysiology and management. Clin. Perinatol. 41, 1–24.

Back, S.A., Miller, S.P., 2014. Brain injury in premature neonates: a primary cerebral dysmaturation disorder? Ann. Neurol. 75, 469–486.

Bassi, L., Ricci, D., Volzone, A., Allsop, J.M., Srinivasan, L., Pai, A., Ribes, C., Ramenghi, L.A., Mercuri, E., Mosca, F., Edwards, A.D., Cowan, F.M., Rutherford, M.A., Counsell, S.J., 2008. Probabilistic diffusion tractography of the optic radiations and visual function in preterm infants at term equivalent age. Brain 131, 573–582.

Behrens, T.E., Berg, H.J., Jbabdi, S., Rushworth, M.F., Woolrich, M.W., 2007. Probabilistic diffusion tractography with multiple fibre orientations: what can we gain? Neuroimage 34, 144–155.

Benjamini, Y., Krieger, A.M., Yekutieli, D., 2006. Adaptive linear step-up procedures that control the false discovery rate. Biometrika 93, 491–507.

Bjuland, K.J., Lohaugen, G.C., Martinussen, M., Skranes, J., 2013. Cortical thickness and cognition in very-low-birth-weight late teenagers. Early Hum. Dev. 89, 371–380.

Boretius, S., Escher, A., Dallenga, T., Wrzos, C., Tammer, R., Bruck, W., Nessler, S., Frahm, J., Stadelmann, C., 2012. Assessment of lesion pathology in a new animal model of MS by multiparametric MRI and DTI. Neuroimage 59, 2678–2688.

Buser, J.R., Maire, J., Riddle, A., Gong, X., Nguyen, T., Nelson, K., Luo, N.L., Ren, J., Struve, J., Sherman, L.S., Miller, S.P., Chau, V., Hendson, G., Ballabh, P., Grafe, M.R., Back, S.A., 2012. Arrested preoligodendrocyte maturation contributes to myelination failure in premature infants. Ann. Neurol. 71, 93–109.

Callaway, E.M., Borrell, V., 2011. Developmental sculpting of dendritic morphology of layer 4 neurons in visual cortex: influence of retinal input. J. Neurosci. 31, 7456–7470.

Cheong, J.L., Thompson, D.K., Wang, H.X., Hunt, R.W., Anderson, P.J., Inder, T.E., Doyle, L.W., 2009. Abnormal white matter signal on MR imaging is related to abnormal tissue microstructure. AJNR Am J Neuroradiol 30, 623–628.

Constable, R.T., Ment, L.R., Vohr, B.R., Kesler, S.R., Fulbright, R.K., Lacadie, C., Delancy, S., Katz, K.H., Schneider, K.C., Schafer, R.J., Makuch, R.W., Reiss, A.R., 2008. Prematurely born children demonstrate white matter microstructural differences at 12 years of age, relative to term control subjects: an investigation of group and gender effects. Pediatrics 121, 306–316.

Counsell, S.J., Dyet, L.E., Larkman, D.J., Nunes, R.G., Boardman, J.P., Allsop, J.M., Fitzpatrick, J., Srinivasan, L., Cowan, F.M., Hajnal, J.V., Rutherford, M.A., Edwards, A.D., 2007. Thalamo-cortical connectivity in children born preterm mapped using probabilistic magnetic resonance tractography. Neuroimage 34, 896–904.

Counsell, S.J., Edwards, A.D., Chew, A.T., Anjari, M., Dyet, L.E., Srinivasan, L., Boardman, J.P., Allsop, J.M., Hajnal, J.V., Rutherford, M.A., Cowan, F.M., 2008. Specific relations between neurodevelopmental abilities and white matter microstructure in children born preterm. Brain 131, 3201–3208.

Dale, A.M., Fischl, B., Sereno, M.I., 1999. Cortical surface-based analysis: I. Segmentation and surface reconstruction. Neuroimage 9, 179–194.
Dale, A.M., Sereno, M.I., 1993. Improved localization of cortical activity by combining EEG and MEG with MRI cortical surface reconstruction - a linear-approach. J. Cognit. Neurosci. 5, 162–176.
De Santis, S., Drakesmith, M., Bells, S., Assaf, Y., Jones, D.K., 2014. Why diffusion tensor MRI does well only some of the time: variance and covariance of white matter tissue microstructure attributes in the living human brain. Neuroimage 89, 35–44.
Dean, J.M., Bennet, L., Back, S.A., McClendon, E., Riddle, A., Gunn, A.J., 2014. What brakes the preterm brain? An arresting story. Pediatr. Res. 75, 227–233.
Dean, J.M., McClendon, E., Hansen, K., Azimi-Zonooz, A., Chen, K., Riddle, A., Gong, X., Sharifnia, E., Hagen, M., Ahmad, T., Leigland, L.A., Hohimer, A.R., Kroenke, C.D., Back, S.A., 2013. Prenatal cerebral ischemia disrupts MRI-defined cortical microstructure through disturbances in neuronal arborization. Sci. Transl. Med. 5, 168ra167.
Dick, A.S., Tremblay, P., 2012. Beyond the arcuate fasciculus: consensus and controversy in the connectional anatomy of language. Brain 135, 3529–3550.
Douaud, G., Jbabdi, S., Behrens, T.E., Menke, R.A., Gass, A., Monsch, A.U., Rao, A., Whitcher, B., Kindlmann, G., Matthews, P.M., Smith, S., 2011. DTI measures in crossing-fibre areas: increased diffusion anisotropy reveals early white matter alteration in MCI and mild Alzheimer's disease. Neuroimage 55, 880–890.
Eikenes, L., Lohaugen, G.C., Brubakk, A.M., Skranes, J., Haberg, A.K., 2011. Young adults born preterm with very low birth weight demonstrate widespread white matter alterations on brain DTI. Neuroimage 54, 1774–1785.
Feldman, H.M., Lee, E.S., Yeatman, J.D., Yeom, K.W., 2012. Language and reading skills in school-aged children and adolescents born preterm are associated with white matter properties on diffusion tensor imaging. Neuropsychologia 50, 3348–3362.
Fischl, B., Dale, A.M., 2000. Measuring the thickness of the human cerebral cortex from magnetic resonance images. Proc. Natl. Acad. Sci. U. S. A. 97, 11050–11055.
Fischl, B., Liu, A., Dale, A.M., 2001. Automated manifold surgery: constructing geometrically accurate and topologically correct models of the human cerebral cortex. IEEE Trans. Med. Imag. 20, 70–80.
Fischl, B., Salat, D.H., Busa, E., Albert, M., Dieterich, M., Haselgrove, C., van der Kouwe, A., Killiany, R., Kennedy, D., Klaveness, S., Montillo, A., Makris, N., Rosen, B., Dale, A.M., 2002. Whole brain segmentation: automated labeling of neuroanatomical structures in the human brain. Neuron 33, 341–355.
Fischl, B., Salat, D.H., van der Kouwe, A.J., Makris, N., Segonne, F., Quinn, B.T., Dale, A.M., 2004a. Sequence-independent segmentation of magnetic resonance images. Neuroimage 23 (Suppl. 1), S69–S84.
Fischl, B., Sereno, M.I., Dale, A.M., 1999a. Cortical surface-based analysis: II: inflation, flattening, and a surface-based coordinate system. Neuroimage 9, 195–207.
Fischl, B., Sereno, M.I., Tootell, R.B., Dale, A.M., 1999b. High-resolution intersubject averaging and a coordinate system for the cortical surface. Hum. Brain Mapp. 8, 272–284.
Fischl, B., van der Kouwe, A., Destrieux, C., Halgren, E., Segonne, F., Salat, D.H., Busa, E., Seidman, L.J., Goldstein, J., Kennedy, D., Caviness, V., Makris, N., Rosen, B., Dale, A.M., 2004b. Automatically parcellating the human cerebral cortex. Cerebr. Cortex 14, 11–22.
Giedd, J.N., 2004. Structural magnetic resonance imaging of the adolescent brain. Ann. N. Y. Acad. Sci. 1021, 77–85.
Gimenez, M., Miranda, M.J., Born, A.P., Nagy, Z., Rostrup, E., Jernigan, T.L., 2008. Accelerated cerebral white matter development in preterm infants: a voxel-based morphometry study with diffusion tensor MR imaging. Neuroimage 41, 728–734.
Goldman-Rakic, P.S., Bourgeosis, J.-P., Rakic, P., 1997. Development of the prefrontal cortex evolution, neuorbiology and behaviour. In: Krasnegor, N., Lyon, G., Goldman-Rakic, P.S. (Eds.), Synaptic Substratee of Cognitive Development: Life-span Analysis of Synaptogenesis in the Preforntal Cortex of Nonhuman Primate, pp. 27–47.
Groeschel, S., Tournier, J.D., Northam, G.B., Baldeweg, T., Wyatt, J., Vollmer, B., Connelly, A., 2014. Identification and interpretation of microstructural abnormalities in motor pathways in adolescents born preterm. Neuroimage 87, 209–219.
Hamrick, S.E., Miller, S.P., Leonard, C., Glidden, D.V., Goldstein, R., Ramaswamy, V., Piecuch, R., Ferriero, D.M., 2004. Trends in severe brain injury and neurodevelopmental outcome in premature newborn infants: the role of cystic periventricular leukomalacia. J. Pediatr. 145, 593–599.
Hollingshead, A.B., 1957. Two Factor Index of Social Position. Mimeo. Yale University, New Haven, Connecticut.
Huppi, P.S., Murphy, B., Maier, S.E., Zientara, G.P., Inder, T.E., Barnes, P.D., Kikinis, R., Jolesz, F.A., Volpe, J.J., 2001. Microstructural brain development after perinatal cerebral white matter injury assessed by diffusion tensor magnetic resonance imaging. Pediatrics 107, 455–460.
Huppi, P.S., Warfield, S., Kikinis, R., Barnes, P.D., Zientara, G.P., Jolesz, F.A., Tsuji, M.K., Volpe, J.J., 1998. Quantitative magnetic resonance imaging of brain development in premature and mature newborns. Ann. Neurol. 43, 224–235.
Huttenlocher, P.R., 1979. Synaptic density in human frontal cortex - developmental changes and effects of aging. Brain Res. 163, 195–205.
Indredavik, M.S., Vik, T., Heyerdahl, S., Kulseng, S., Fayers, P., Brubakk, A.M., 2004. Psychiatric symptoms and disorders in adolescents with low birth weight. Arch. Dis. Child. Fetal Neonatal Ed. 89, F445–F450.
Jeon, T., Mishra, V., Ouyang, M., Chen, M., Huang, H., 2015. Synchronous changes of cortical thickness and corresponding white matter microstructure during brain development accessed by diffusion MRI tractography from parcellated cortex. Front. Neuroanat. 9, 158.
Jeurissen, B., Leemans, A., Tournier, J.D., Jones, D.K., Sijbers, J., 2013. Investigating the prevalence of complex fiber configurations in white matter tissue with diffusion magnetic resonance imaging. Hum. Brain Mapp. 34, 2747–2766.
Jones, D.K., 2010. Challenges and limitations of quantifying brain connectivity in vivo with diffusion MRI. Imag. Med. 2, 341–355.
Jurcoane, A., Daamen, M., Scheef, L., Bauml, J.G., Meng, C., Wohlschlager, A.M., Sorg, C., Busch, B., Baumann, N., Wolke, D., Bartmann, P., Hattingen, E., Boecker, H., 2016. White matter alterations of the corticospinal tract in adults born very preterm and/or with very low birth weight. Hum. Brain Mapp. 37, 289–299.
Løhaugen, G.C., Gramstad, A., Evensen, K.A., Martinussen, M., Lindqvist, S., Indredavik, M., Vik, T., Brubakk, A.M., Skranes, J., 2010. Cognitive profile in young adults born preterm at very low birthweight. Dev. Med. Child Neurol. 52, 1133–1138.
MacKinnon, D.P., Dwyer, J.H., 1993. Estimating mediated effects in prevention studies. Eval. Rev. 17, 144–158.
Marin-Padilla, M., 1997. Developmental neuropathology and impact of perinatal brain damage. II: white matter lesions of the neocortex. J. Neuropathol. Exp. Neurol. 56, 219–235.
Martinussen, M., Fischl, B., Larsson, H.B., Skranes, J., Kulseng, S., Vangberg, T.R., Vik, T., Brubakk, A.M., Haraldseth, O., Dale, A.M., 2005. Cerebral cortex thickness in 15-year-old adolescents with low birth weight measured by an automated MRI-based method. Brain 128, 2588–2596.
McAllister, A.K., Katz, L.C., Lo, D.C., 1996. Neurotrophin regulation of cortical dendritic growth requires activity. Neuron 17, 1057–1064.
McMillen, I.C., Adams, M.B., Ross, J.T., Coulter, C.L., Simonetta, G., Owens, J.A., Robinson, J.S., Edwards, L.J., 2001. Fetal growth restriction: adaptations and consequences. Reproduction 122, 195–204.
Mullen, K.M., Vohr, B.R., Katz, K.H., Schneider, K.C., Lacadie, C., Hampson, M., Makuch, R.W., Reiss, A.L., Constable, R.T., Ment, L.R., 2011. Preterm birth results in alterations in neural connectivity at age 16 years. Neuroimage 54, 2563–2570.
Muthén, L.K., Muthén, B.O., 1998-2011. Mplus User's Guide, sixth ed. Muthén & Muthén, Los Angeles, CA.
Nagy, Z., Westerberg, H., Skare, S., Andersson, J.L., Lilja, A., Flodmark, O., Fernell, E., Holmberg, K., Bohm, B., Forssberg, H., Lagercrantz, H., Klingberg, T., 2003. Preterm children have disturbances of white matter at 11 years of age as shown by diffusion tensor imaging. Pediatr. Res. 54, 672–679.
Nam, K.W., Castellanos, N., Simmons, A., Froudist-Walsh, S., Allin, M.P., Walshe, M., Murray, R.M., Evans, A., Muehlboeck, J.S., Nosarti, C., 2015. Alterations in cortical thickness development in preterm-born individuals: implications for high-order cognitive functions. Neuroimage 115, 64–75.
Oh, J.B., Lee, S.K., Kim, K.K., Song, I.C., Chang, K.H., 2004. Role of immediate postictal diffusion-weighted MRI in localizing epileptogenic foci of mesial temporal lobe epilepsy and non-lesional neocortical epilepsy. Seizure 13, 509–516.
Oishi, K., Mori, S., Donohue, P.K., Ernst, T., Anderson, L., Buchthal, S., Faria, A., Jiang, H., Li, X., Miller, M.I., van Zijl, P.C., Chang, L., 2011. Multi-contrast human neonatal brain atlas: application to normal neonate development analysis. Neuroimage 56, 8–20.
Olsen, A., Dennis, E.L., Evensen, K.A.I., Husby Hollund, I.M., Lohaugen, G.C.C., Thompson, P.M., Brubakk, A.M., Eikenes, L., Haberg, A.K., 2018. Preterm birth leads to hyper-reactive cognitive control processing and poor white matter organization in adulthood. Neuroimage 167, 419–428.
Papagno, C., 2011. Naming and the role of the uncinate fasciculus in language function. Curr. Neurol. Neurosci. Rep. 11, 553–559.
Partridge, S.C., Mukherjee, P., Henry, R.G., Miller, S.P., Berman, J.I., Jin, H., Lu, Y., Glenn, O.A., Ferriero, D.M., Barkovich, A.J., Vigneron, D.B., 2004. Diffusion tensor imaging: serial quantitation of white matter tract maturity in premature newborns. Neuroimage 22, 1302–1314.
Petanjek, Z., Judas, M., Simic, G., Rasin, M.R., Uylings, H.B., Rakic, P., Kostovic, I., 2011. Extraordinary neoteny of synaptic spines in the human prefrontal cortex. Proc. Natl. Acad. Sci. U. S. A. 108, 13281–13286.
Pierson, C.R., Folkerth, R.D., Billiards, S.S., Trachtenberg, F.L., Drinkwater, M.E., Volpe, J.J., Kinney, H.C., 2007. Gray matter injury associated with periventricular leukomalacia in the premature infant. Acta Neuropathol. 114, 619–631.
Pollack, R.N., Divon, M.Y., 1992. Intrauterine growth retardation: definition, classification, and etiology. Clin. Obstet. Gynecol. 35, 99–107.
Rakic, P., 1988. Specification of cerebral cortical areas. Science 241, 170–176.
Rimol, L.M., Bjuland, K.J., Lohaugen, G.C., Martinussen, M., Evensen, K.A., Indredavik, M.S., Brubakk, A.M., Eikenes, L., Haberg, A.K., Skranes, J., 2016. Cortical trajectories during adolescence in preterm born teenagers with very low birthweight. Cortex 75, 120–131.
Rose, S.E., Hatzigeorgiou, X., Strudwick, M.W., Durbridge, G., Davies, P.S., Colditz, P.B., 2008. Altered white matter diffusion anisotropy in normal and preterm infants at term-equivalent age. Magn. Reson. Med. 60, 761–767.
Schaeffer, D.J., Krafft, C.E., Schwarz, N.F., Chi, L., Rodrigue, A.L., Pierce, J.E., Allison, J.D., Yanasak, N.E., Liu, T., Davis, C.L., McDowell, J.E., 2014. The relationship between uncinate fasciculus white matter integrity and verbal memory proficiency in children. Neuroreport 25, 921–925.
Sidman, R.L., Rakic, P., 1973. Neuronal migration, with special reference to developing human brain: a review. Brain Res. 62, 1–35.
Skranes, J., Lohaugen, G.C., Martinussen, M., Haberg, A., Brubakk, A.M., Dale, A.M., 2013. Cortical surface area and IQ in very-low-birth-weight (VLBW) young adults. Cortex 49, 2264–2271.
Skranes, J., Lohaugen, G.C., Martinussen, M., Indredavik, M.S., Dale, A.M., Haraldseth, O., Vangberg, T.R., Brubakk, A.M., 2009. White matter abnormalities and executive function in children with very low birth weight. Neuroreport 20, 263–266.
Skranes, J., Vangberg, T.R., Kulseng, S., Indredavik, M.S., Evensen, K.A., Martinussen, M., Dale, A.M., Haraldseth, O., Brubakk, A.M., 2007. Clinical findings and white matter

abnormalities seen on diffusion tensor imaging in adolescents with very low birth weight. Brain 130, 654–666.
Song, S.K., Sun, S.W., Ju, W.K., Lin, S.J., Cross, A.H., Neufeld, A.H., 2003. Diffusion tensor imaging detects and differentiates axon and myelin degeneration in mouse optic nerve after retinal ischemia. Neuroimage 20, 1714–1722.
Song, S.K., Sun, S.W., Ramsbottom, M.J., Chang, C., Russell, J., Cross, A.H., 2002. Dysmyelination revealed through MRI as increased radial (but unchanged axial) diffusion of water. Neuroimage 17, 1429–1436.
Sølsnes, A.E., Grunewaldt, K.H., Bjuland, K.J., Stavnes, E.M., Bastholm, I.A., Aanes, S., Ostgard, H.F., Haberg, A., Lohaugen, G.C., Skranes, J., Rimol, L.M., 2015a. Cortical morphometry and IQ in VLBW children without cerebral palsy born in 2003-2007. Neuroimage Clin 8, 193–201.
Sølsnes, A.E., Sripada, K., Yendiki, A., Bjuland, K.J., Ostgard, H.F., Aanes, S., Grunewaldt, K.H., Lohaugen, G.C., Eikenes, L., Haberg, A.K., Rimol, L.M., Skranes, J., 2015b. Limited microstructural and connectivity deficits despite subcortical volume reductions in school-aged children born preterm with very low birth weight. Neuroimage 130, 24–34.
Thomason, M.E., Scheinost, D., Manning, J.H., Grove, L.E., Hect, J., Marshall, N., Hernandez-Andrade, E., Berman, S., Pappas, A., Yeo, L., Hassan, S.S., Constable, R.T., Ment, L.R., Romero, R., 2017. Weak functional connectivity in the human fetal brain prior to preterm birth. Sci. Rep. 7, 39286.
Travis, K.E., Adams, J.N., Ben-Shachar, M., Feldman, H.M., 2015. Decreased and increased anisotropy along major cerebral white matter tracts in preterm children and adolescents. PloS One 10 e0142860.
Travis, K.E., Adams, J.N., Kovachy, V.N., Ben-Shachar, M., Feldman, H.M., 2017. White matter properties differ in 6-year old Readers and Pre-readers. Brain Struct. Funct. 222, 1685–1703.
Tuch, D.S., Salat, D.H., Wisco, J.J., Zaleta, A.K., Hevelone, N.D., Rosas, H.D., 2005. Choice reaction time performance correlates with diffusion anisotropy in white matter pathways supporting visuospatial attention. Proc. Natl. Acad. Sci. U. S. A. 102, 12212–12217.
Valeri, L., Vanderweele, T.J., 2013. Mediation analysis allowing for exposure-mediator interactions and causal interpretation: theoretical assumptions and implementation with SAS and SPSS macros. Psychol. Methods 18, 137–150.
van Tilborg, E., Heijnen, C.J., Benders, M.J., van Bel, F., Fleiss, B., Gressens, P., Nijboer, C.H., 2016. Impaired oligodendrocyte maturation in preterm infants: potential therapeutic targets. Prog. Neurobiol. 136, 28–49.
Vangberg, T.R., Skranes, J., Dale, A.M., Martinussen, M., Brubakk, A.M., Haraldseth, O., 2006. Changes in white matter diffusion anisotropy in adolescents born prematurely. Neuroimage 32, 1538–1548.
Volpe, J.J., 2008. Postnatal sepsis, necrotizing entercolitis, and the critical role of systemic inflammation in white matter injury in premature infants. J. Pediatr. 153, 160–163.
Volpe, J.J., 2009. Brain injury in premature infants: a complex amalgam of destructive and developmental disturbances. Lancet Neurol. 8, 110–124.
Von Der Heide, R.J., Skipper, L.M., Klobusicky, E., Olson, I.R., 2013. Dissecting the uncinate fasciculus: disorders, controversies and a hypothesis. Brain 136, 1692–1707.
Wechsler, D., Nyman, H., Nordvik, H., 2003. Wais-iii: Wechsler Adult Intelligence Scale : Manual. Psykologiförlaget, Stockholm.
Winkler, A.M., Greve, D.N., Bjuland, K.J., Nichols, T.E., Sabuncu, M.R., Håberg, A.K., Skranes, J., Rimol, L.M., 2017. Joint analysis of cortical area and thickness as a replacement for the analysis of the volume of the cerebral cortex. Cerebr. Cortex 1–12.
Yendiki, A., Koldewyn, K., Kakunoori, S., Kanwisher, N., Fischl, B., 2013. Spurious group differences due to head motion in a diffusion MRI study. Neuroimage 88C, 79–90.
Yendiki, A., Panneck, P., Srinivasan, P., Stevens, A., Zollei, L., Augustinack, J., Wang, R., Salat, D., Ehrlich, S., Behrens, T., Jbabdi, S., Gollub, R., Fischl, B., 2011. Automated probabilistic reconstruction of white-matter pathways in health and disease using an atlas of the underlying anatomy. Front. Neuroinf. 5, 23.
Yung, A., Poon, G., Qiu, D.Q., Chu, J., Lam, B., Leung, C., Goh, W., Khong, P.L., 2007. White matter volume and anisotropy in preterm children: a pilot study of neurocognitive correlates. Pediatr. Res. 61, 732–736.